



Surface integrity evaluation within dry grinding process on automotive gears

Flavia Lerra^{a,*}, Francesco Grippo^b, Enrico Landi^b, Alessandro Fortunato^a

^a University of Bologna, Viale Risorgimento 2, 40136, Bologna, Italy

^b SAMPUTensili Machinetools, Bentivoglio, Bologna, Italy

ARTICLE INFO

Keywords:

Dry grinding

Gears

Automotive transmissions

Sustainable technology

ABSTRACT

Gears are essential components in automotive transmissions and their performance directly depends on the flanks surface integrity. To date the gears whole production chain do not use lubricants, except the final step of finishing which adopts a huge amount of oil yet. Sustainability represents a duty and a challenge for the current manufacturing lines, therefore the elimination of oil during the grinding phase represents an alternative in the gears production chain. The main critical aspect is represented by the occurrence of grinding burns that become more likely with the absence of oil. Even if dimensional tolerances and roughness requirements could be respected, the presence of the white and dark layer, due to an excessive heat generation during grinding, reduce the mechanical surface performance and could lead to crack formation and the gear rejection. Some recent studies showed the feasibility of the gear dry grinding, but further investigations must be developed to enrich the knowledge and optimize the process. In this paper gear dry grinding tests were performed and the application of different process parameters, such as grinding wheels, feed rate and number of passes was investigated in terms of surface integrity. Beyond dimensional tolerances and roughness measurements, microstructural analysis through optical microscope and scanning electron microscope (SEM) were executed to effectively define the process configurations feasibility showing that the wheel binder hardness has more impact than porosity in dry grinding microstructural outcomes.

1. Introduction

Electrification in the automotive powertrain has led to a reduction in gears production, especially in the battery electrical vehicles. Even though electric vehicles are expanding widely, a number of transmissions type is produced in the actual powertrain cars market, from the manual and the automated manual to the automatic and the dual clutch transmissions (Kotthoff 2018) where the number of gears required is still high. Therefore, to make the gears production chain more sustainable becomes mandatory. Different actions could be identified to achieve this goal, for instance, material saving by reducing waste and reduction in the use of mineral-based cutting fluids could lead to a cleaner gear manufacturing route. Potential single stage manufacturing of gears are represented by wire electric discharge machining (WEDM) and gear rolling (Gupta et al., 2016). Nowadays, grinding continues to use huge amount of lubricant because it involves the highest specific energy values among machining processes during the material removal phase

(Oliveira et al., 2009), but different technologies which reduce oils such as minimum quantity lubrication (MQL) technique represents an efficient alternative for gear finishing (De Sampaio Alves et al. 2017). The high energy consumption during a grinding operation is mainly due to grains non-deterministic shape with negative cutting angles and the limited depth of cut. The process energy during the removal action is distributed in three different deformation zones which respectively involve elastic and plastic deformation up to the cutting phase (Chen et al. 2017). The first two phenomena release the main part of thermal energy into the workpiece surface due to friction prior to onset of cutting. Therefore, the primary technological role of lubricant is to remove thermal energy from the contact zone. In the last few years, another sustainable gear finishing process is evolving with remarkable feedback: gear dry grinding. The elimination of oil showed a substantial reduction in costs and environmental pollution while keeping the gears standard requirement high (Guerrini et al., 2019). Gear dry grinding process was recently developed (Landi 2016) and aimed to minimize the material

* Corresponding author.

E-mail addresses: flavia.lerra2@unibo.it (F. Lerra), f.grippo@samputensili.it (F. Grippo), e.landi@samputensili.it (E. Landi), alessandro.fortunato@unibo.it (A. Fortunato).

<https://doi.org/10.1016/j.clet.2022.100522>

Received 31 May 2021; Received in revised form 16 May 2022; Accepted 9 June 2022

Available online 15 June 2022

2666-7908/© 2022 The Authors. Published by Elsevier Ltd. This is an open access article under the CC BY license (<http://creativecommons.org/licenses/by/4.0/>).



Fig. 1. SG 160 Sky Grind machine work area configuration.

removed during the grinding by previously introducing, in the same finishing step, a defined skive-hobbing phase which removes at the least the 90% of material allowance. In dry grinding mode the thermal effect on the material ground becomes stronger and if excessive heat is generated in the workpiece, it may be damaged or burned as thermal overloading leads to microstructural changes and degradation of surface integrity (Mayer and Pepi, 2002). Grinding burns are generally identified in softening phenomena, which is characterized by a darkened microstructure and a decrease in mechanical properties, and in severe thermal damage caused by a raise of the temperature above the austenitization temperature which leads to the formation of a white layer and an increase in the surface brittleness which could cause cracks formation (Guerrini et al., 2018). The white layer is formed by a rapid austenite transformation and quenching process, instead the dark softening layer is formed by a tempering process. The plastic deformation generated during the grinding, especially in a dry grinding process, contribute to the grain refinement of both the white and dark layer (Zhang et al., 2018). Different techniques were used to detect gear grinding burns (He et al., 2019) and they involved beforehand prediction methods and post-mortem detection method, but microstructural analysis represents the most univocal strategy which clearly shows the thermal effect caused by the grinding wheel pass on the material (Guerrini et al., 2019b). Grinding process can be considered as a thermal cycle so it depends on the process parameters and material involved, but also on the contact time which directly affect the temperature reached in the surface during the operation (Jermolajev et al. 2018). Due to the severe heat cycle, the time-dependent transformation occurs at different temperature and time compared to the conventional transformation, introducing the concept of the “overheating” for severe heat-cycle transformation (Liverani et al., 2017). Thermal damage is therefore caused by a severe plastic deformation and a rapid local heating rate which induce high superheat and provide sufficient phase transformation mechanism. Beyond the microstructural requirement, gear hard finishing have to achieve the maximum load capacity and the minimum running noise, therefore, the related measures on geometric flank modifications and reduction of form errors have to be carefully respected (Karpuschewski et al. 2008). Among the surface integrity parameters, also roughness and surface topography exerts a significant influence on the component performance, such as fatigue life (Mallipeddi et al., 2019), contact, wear, tribology, and lubrication (Zhou et al. 2020), therefore, it is of considerable significance to analyze overall the gear profile integrity. As the surface characteristics by a hard finishing process have a decisive influence on the performance of gears, to meet the increasing demand for service performance and fatigue life of gears, the surface integrity analysis has become a critical mechanical scientific challenge. The present study aimed to analyze the surface integrity on dry ground gears through the application of different grinding wheels and process parameters in a real industrial environment taking into account the macro geometrical features also. Two different wheel specifications were adopted, a fused aluminum oxide and a silicon carbide grinding wheel with a grain size of 120. Dry grinding tests were

Table 1
Characteristics of gear.

Parameter	Value
Normal module m	1.8 mm
Maximum roughness R_a	0.6 μm
Maximum profile form error $ff\alpha$	6 μm
Maximum helix form error $ff\beta$	5.5 μm
Helix crowning range $c\beta$	4 \pm 2 μm

Table 2
Characteristics of grinding wheels.

Parameter	Wheel 1	Wheel 2
Diameter D_w	250 mm	250 mm
Width b_w	100 mm	100 mm
No. starts	4	4
Abrasive grain material	Fused aluminum oxide	Silicon carbide
Grit size	120	120
Binder type	Vitrified	Vitrified
Binder hardness	H	J
Structure	11	18

Table 3
Dry grinding process parameters.

Parameter	Set up 1	Set up 2	Set up 3	Set up 4	Set up 5
Grinding wheel	Wheel 1	Wheel 1	Wheel 1	Wheel 2	Wheel 2
Cutting speed v_t	80 m/s				
Number of passes	1	1	2	1	1
Stock removal p	0.01 mm	0.01 mm	0.005 mm	0.01 mm	0.01 mm
Feed rate f	0.34 mm/rev	0.54 mm/rev	0.34 mm/rev	0.34 mm/rev	0.54 mm/rev
Shifting sh	0.03 mm/mm				

performed using two different feed rate values equal to 0,34 and 0,54 mm/rev and the comparison between single pass and double pass was also evaluated maintaining constant the overall depth of cut. Gears dry grinding feasibility was evaluated by analyzing teeth flanks dimensional tolerances and roughness together with microstructural analysis by means of an optical microscope and SEM analysis. Surface integrity results were correlated to on-line spindle power detections.

2. Material and method

2.1. Experimental set up

Dry grinding tests were performed on a Samputensili SG 160 Sky Grind machine, characterized by the presence of two spindles and designed for automotive mass production (Fig. 1). Gear dry-hard finishing comprises two different steps. A previous skive-hobbing phase which adopts a defined-geometry tool, removes the main allowance on the gear; then a grinding pass allows to obtain the stringent dimensional requirements removing a minimum amount of material reducing the thermal defects risk. An optical sensor promotes the correct phasing of the gear which is positioned on an expansion spindle and rotates with a rotational speed according to the transmission ratio with the wheel.

The reference helical gear represents a typical automotive gear used as the four-six speed of six-speed gearboxes and was made of 27MnCr5. Geometric data were reported in Table 1. After a green turning and the hobbing phase, the gears were heat treated through vacuum carburizing and gas quenching followed by stress relieving in order to reach a surface hardness range of 680–790 HV10.

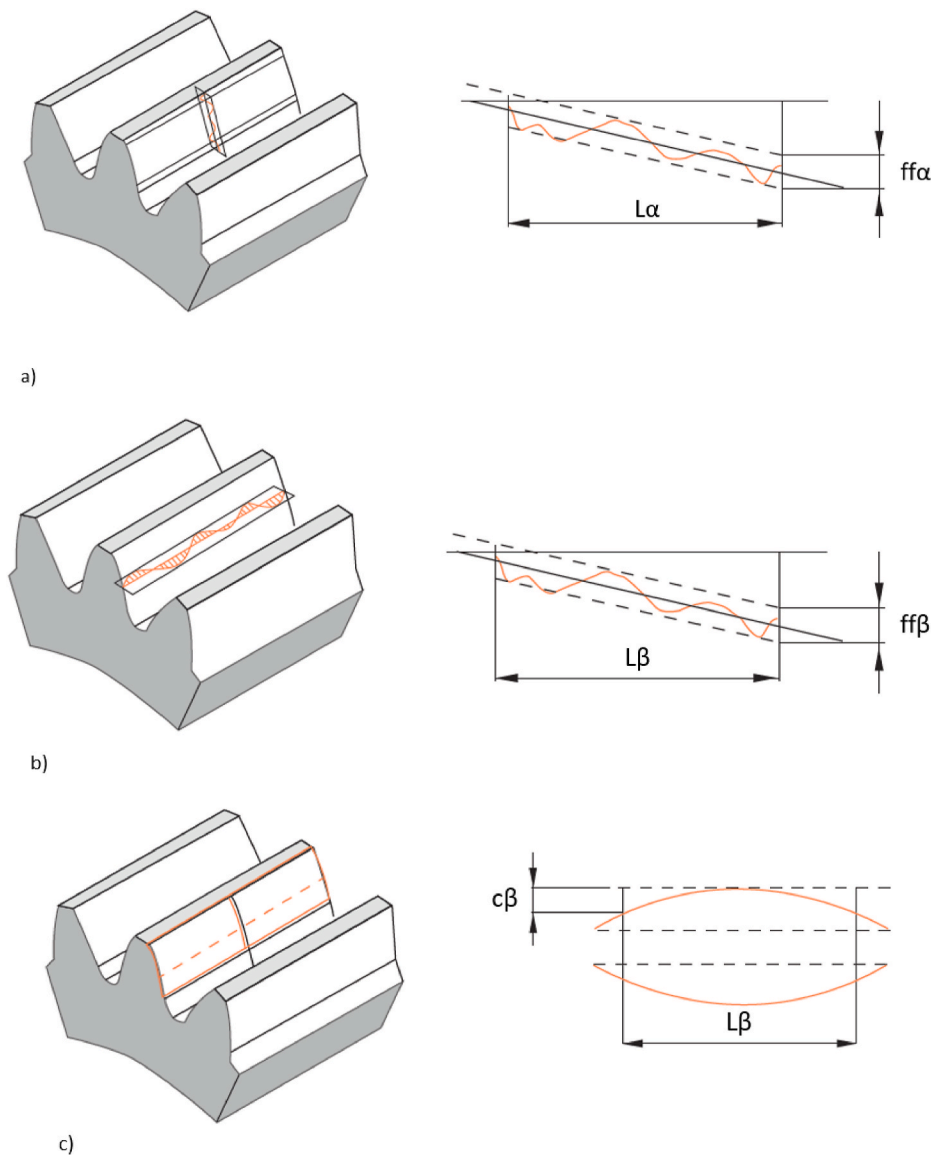


Fig. 2. Definition of profile form deviation $f\phi\alpha$ (a); helix form deviation $f\phi\beta$ (b); helix crowning (c).

Two different grinding wheels characterized by medium binder hardness and different porosity were used to analyze the effect of different grain material and structure in terms of gear quality. Grinding wheel specifications were chosen based on the company experience and their characteristics were reported in Table 2.

In Table 3 the dry grinding cycle parameters used for all the set up were reported. Each grinding cycle was preceded by a skive-hobbing phase which adopted a cutting speed of 2.5 m/s, a stock of 0.09 mm and a feed rate of 2.27 mm/rev. Skiving removed material in up-grinding mode, instead, the grinding wheel was used in down-grinding mode. Grinding tests with the different grinding wheels were performed using two different values of feed rate. Moreover, grinding tests with fused alumina oxide abrasives were developed using single and double pass with fixed compressive stock value. Three repetitions were performed for each test.

2.2. Dimensional analysis

Gear macro and micro-geometric accuracy addressed the deviations in tooth spacing, profile and helix slope, and tooth surface profile and helix roughness and form deviation, respectively. Macro geometry

depends on process kinematics and wheel dressing. Meanwhile, micro geometry is determined by the process parameters. The accuracy of a produced gear, in terms of dimensional tolerances, is identified by comparing the real and the designed geometry. The dimensional tolerances measurements were performed according to AGMA915-1-A02 (AGMA 915-1-A02, 2002) on the flank profile and the flank lead on four diametral distanced teeth on both right and left flank. Dimensional tolerances analysis takes place in a Klingenberg measuring system with the gear placed on a shaft and the contours of the teeth was acquired via a touching probe along the profile and lead directions. In particular, the characteristics considered can be summarized as follows:

1. $f\phi\alpha$ is the profile form deviation and represents the deviation between two lines parallel to the average profile intercepting the highest and the lowest point on the profile in the evaluation field (Fig. 2 a).
2. $f\phi\beta$ is the helix form deviation and represents the deviation between two lines parallel to the average helix intercepting the highest and the lowest point on the profile in the evaluation field (Fig. 2 b).
3. $c\beta$ is the helix crowning and represents the chordal thickness of the tooth along its axis (Fig. 2 c).

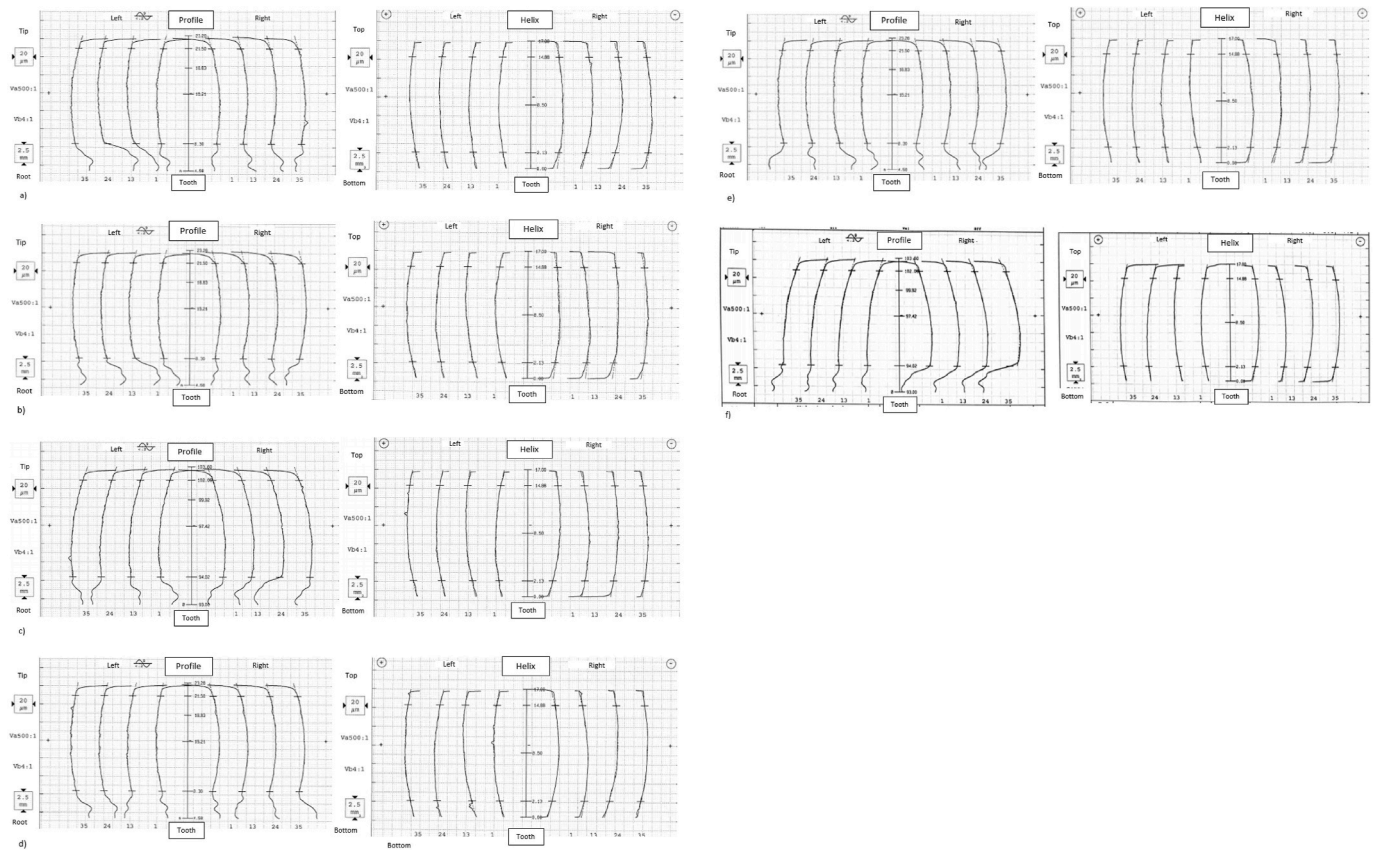


Fig. 3. Dimensional tolerances measurements: set up 1 (a); set up 2 (b); set up 3 (c); set up 4 (d); set up 5 (e); wet griding reference (f).

Measurement of these parameters was carried out on both the right and left flanks and the arithmetic average was calculated to obtain one single value for each parameter and gear.

2.3. Surface integrity analysis

Tooth profile and helix arithmetical mean roughness R_a

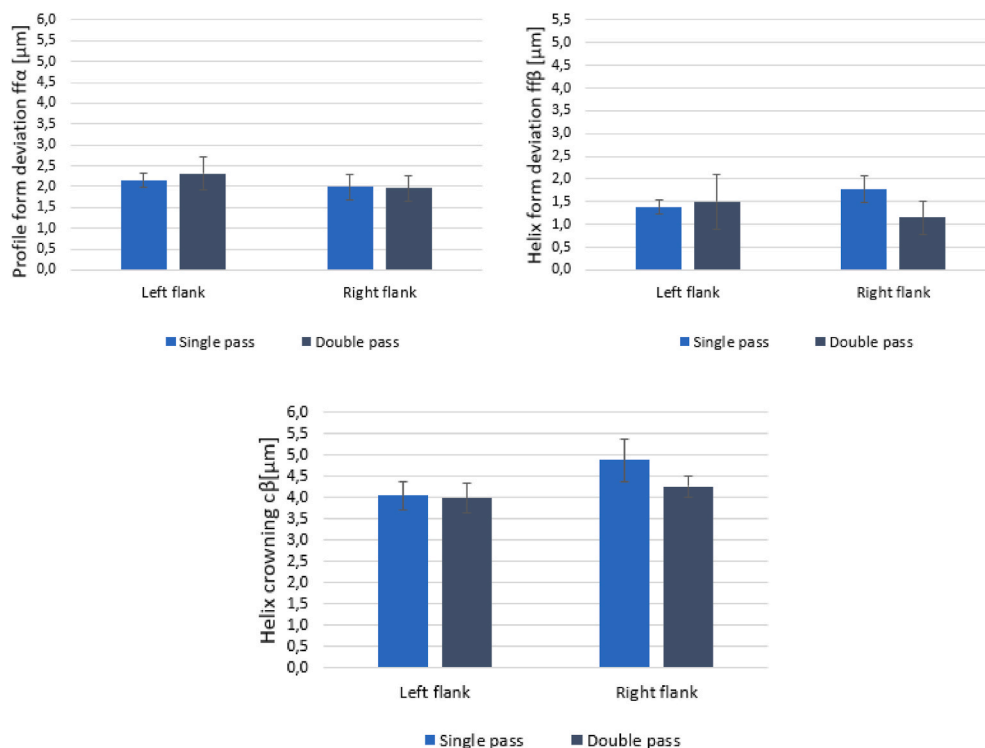


Fig. 4. Profile and helix form deviation and helix crowning comparison between single and double pass.

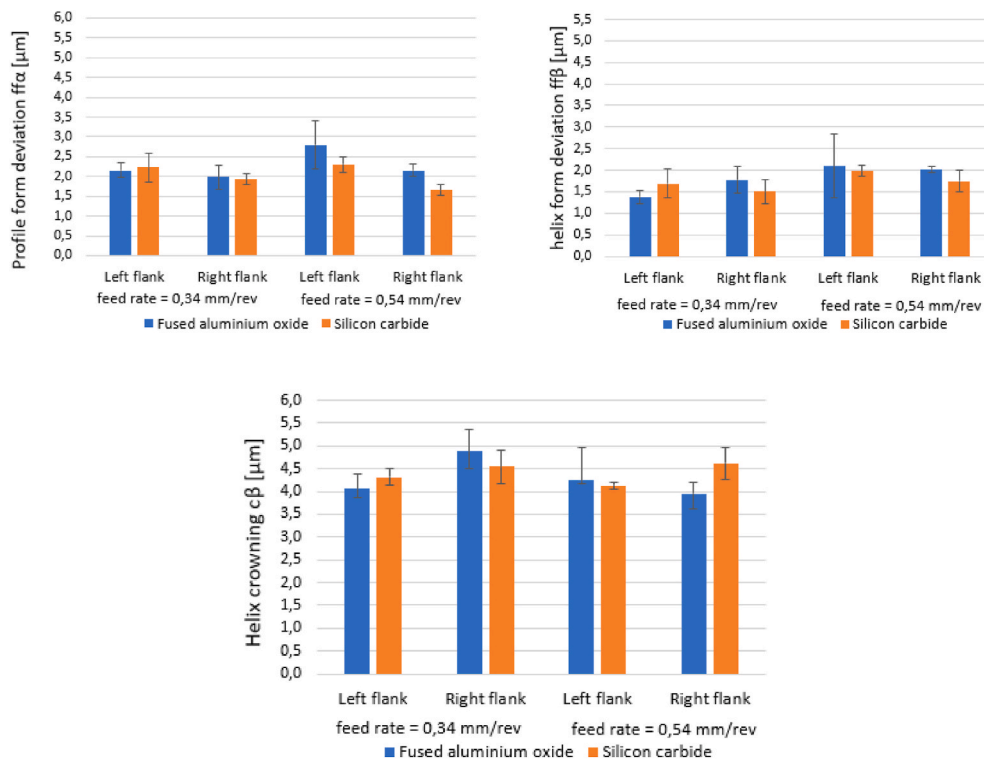


Fig. 5. Profile and helix form deviation and helix crowning comparison between fused aluminium oxide and silicon carbide grinding wheel. (For interpretation of the references to colour in this figure legend, the reader is referred to the Web version of this article.)

measurements were performed on three teeth for each configuration using a Klingenberg P65 measuring system. Roughness values were detected on both right and left flank. Microstructural analysis was carried out with an optical microscope Zeiss Axio Vert.A1M with magnification 20x on the samples prepared according to standard metallographic techniques comprising mechanical grinding (80–2400 grit paper) and polishing with alumina in suspension down to a particle size of 6 to 1 μm. In order to reveal microstructural features, the samples were etched using Nital reagent for 3 s. Microstructural analysis was performed to verify the presence of thermal defects on both right and left flank. A scanning electron microscope equipped with an energy dispersive spectroscope (SEM-EDS) and a field emission gun SEM (FEG-SEM) with a factor magnification of 7 kx was used to observe in detail the surface microstructure and analyze the white layer structure generated on a damaged gear.

3. Results and discussion

3.1. Dimensional tolerances

Measurements were detected by using a standard gear inspection instrument which was set up with the gear geometric requirements

reported in the technical drawing. In Fig. 3 a-e, the shape of the tooth along the profile and the helix as ground were reported for each dry grinding configurations, instead Fig. 3 f showed the reference wet grinding process outcomes. Dimensional measurements showed the shape obtained after grinding on four different teeth equally spaced on both left and right flank. Overall, the graphs showed a smooth and regular shape for all grinding configurations comparable to a reference wet grinding process suggesting a correct finishing phase for each set up from the geometrical point of view.

In Fig. 4 the comparison on the profile and helix form error and the helix crowning between the single and double pass using the fused aluminium oxide wheel was reported. Instead, Fig. 5 showed the same information by comparing the two different grinding wheels with varying feed rate value. The graphs reported the measurements for both right and left flank with the dimensional range reported in Table 1, all the set up respected the tolerances requirements. Considering the comparison between single and double pass, no remarkable differences were shown, except for the helix right flank where the double pass seems to reduce the helix form deviation and crowning.

Regarding the comparison between the different grinding wheels, the silicon carbide wheel was able to maintain the form error deviation lower than the fused aluminium oxide wheel, especially with the higher

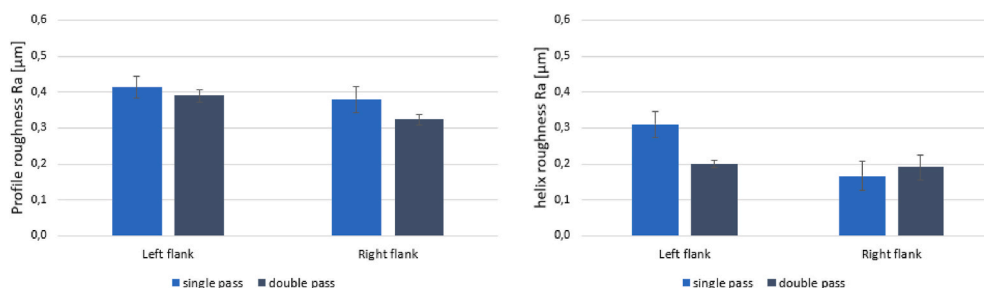


Fig. 6. Profile and helix roughness Ra comparison between single and double pass.

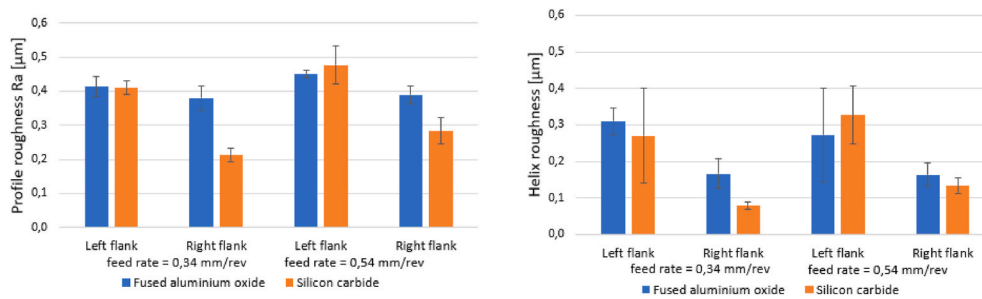


Fig. 7. Profile and helix roughness Ra comparison between fused aluminium oxide and silicon carbide wheel. (For interpretation of the references to colour in this figure legend, the reader is referred to the Web version of this article.)

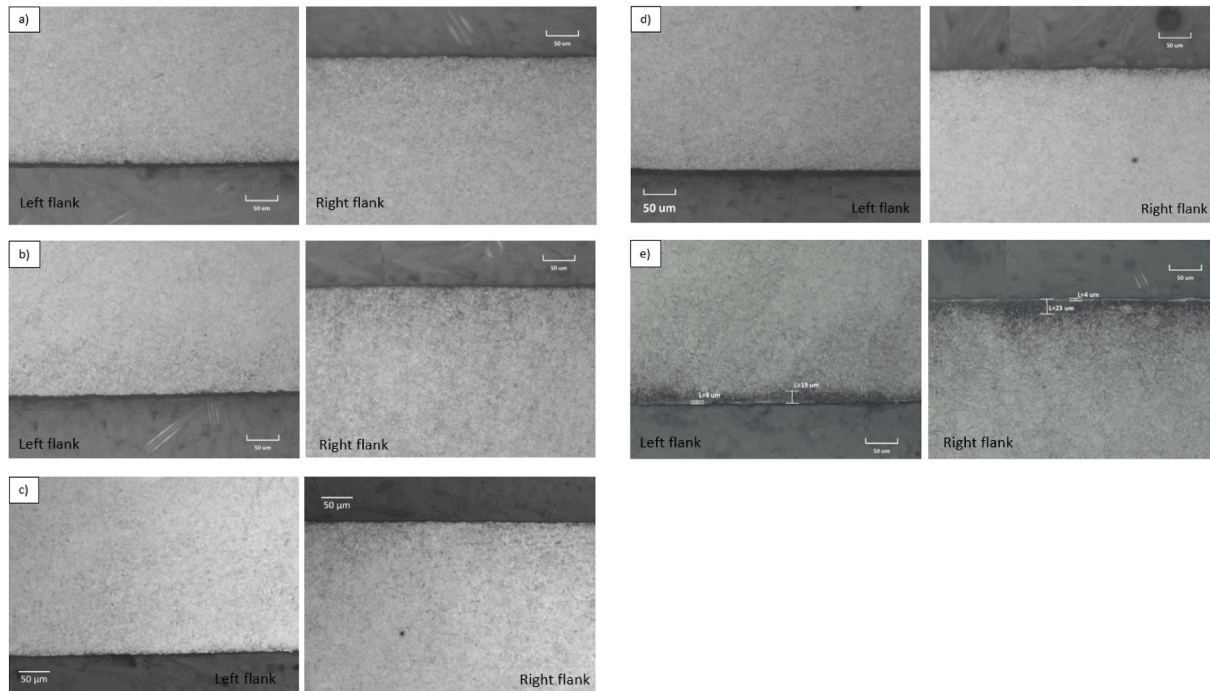


Fig. 8. Optical microscope microstructural analysis: set up 1 (a); set up 2 (b); set up 3 (c); set up 4 (d); set up 5 (e).

feed rate value. However, it can be noticed that on the profile and helix the lower feed rate could reduce the form deviation, but it seems not influencing the helix crowning consistently. According to theory, a lower feed rate allow to reduce micro and macro geometrical deviation being the surface finished with more accuracy. Hence, considering the dimensional analysis, the feed rate parameter has a more relevant role compared to the grinding wheel specification.

3.2. Roughness

Roughness values measured were respected the requirements in all cases. Fig. 6 showed the comparison between single and double pass using the fused aluminium oxide wheel with a constant feed rate of 0,34 mm/rev. For both right and left flank profile and helix, the process adopting the double pass tend to reduce the roughness values, except for the right flank helix. Double pass increases the possibility to flat the asperities left by the previous pass. A slightly difference between the left flank and right flank was visible. Considering the comparison between the grinding wheels and feed rate (Fig. 7) by adopting a single pass, the left flank became more critical than the right one, especially for the silicon carbide wheel, probably due to the wheel dressing procedure. Same dressing parameters were adopted for the grinding wheels, but this phenomenon was marked for the silicon carbide grinding wheel and a

substantial difference between right and left flank roughness was showed. Consequently, silicon carbide wheel reached lower roughness values on the right flank compared to the fused aluminium oxide wheel, instead, roughness values on the left flanks are comparable between the wheels. Considering the effect of feed rate, an increase in the feed rate induces a raise in the roughness, especially on the tooth profile.

3.3. Microstructural analysis

In Fig. 8 a-b the left and right flank microstructure related to the fused aluminium oxide wheel with a feed rate equal to 0,34 and 0,54 mm/rev was respectively shown. Fig. 8 c reported the microstructure of the flanks gear ground with the double pass. The typical martensite structure of the case-hardened depth is visible without remarkable thermal defects in all the above-mentioned cases. Fig. 8 d-e showed the microstructures obtained by the dry grinding process with the silicon carbide wheel. With the lowest feed rate values, the left flank does not present visible marks, instead, the right flank showed a slightly white layer onset. Increasing the feed rate to a value of 0,54 mm/rev, both right and left flank reported visible grinding burns. White and darkened layers were shown with a maximum thickness value of 4 and 25 µm, respectively. Even though, the silicon carbide grinding wheel is characterized by higher porosity level, the higher binder hardness more

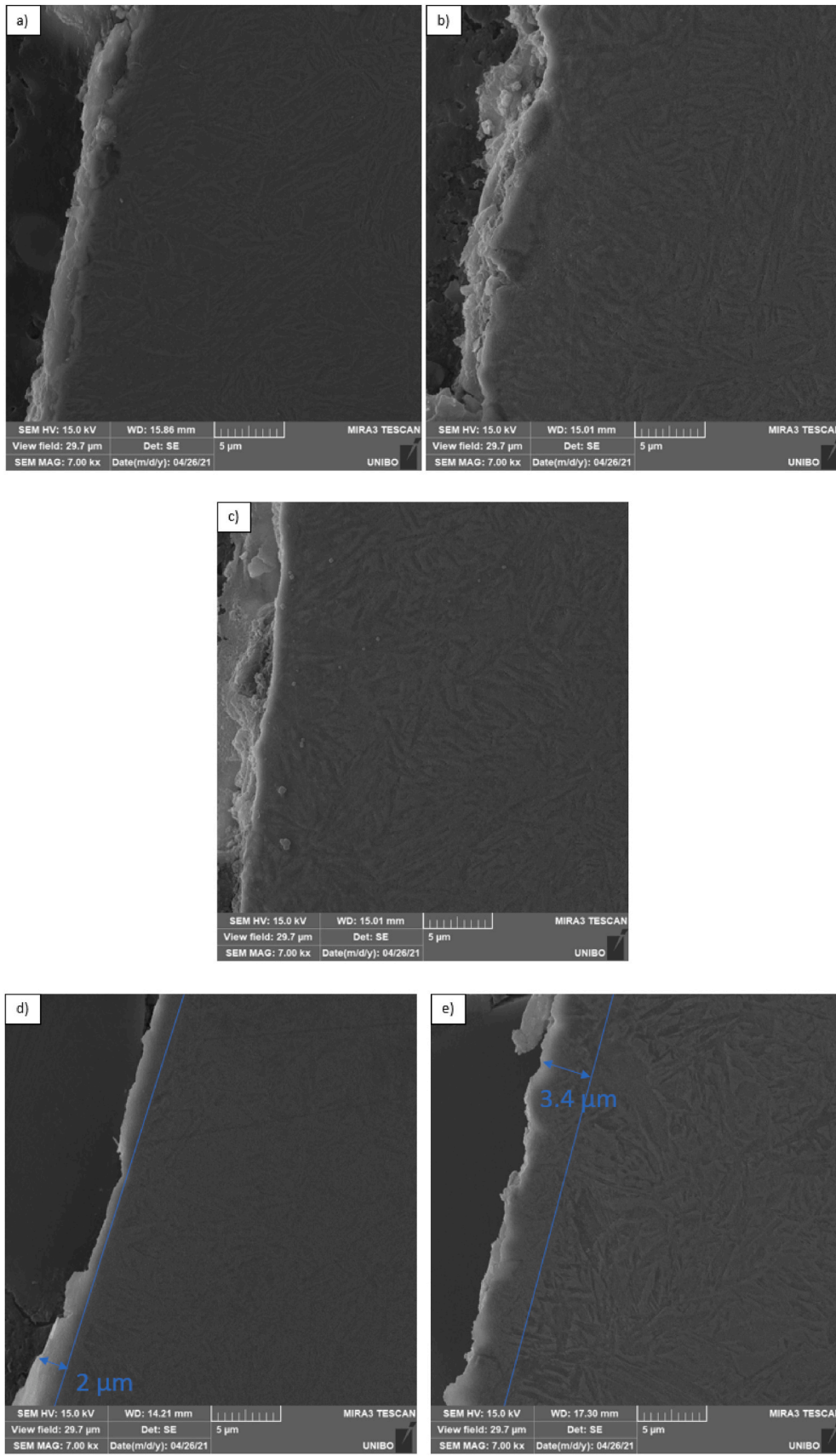


Fig. 9. SEM microstructural analysis: set up 1 (a); set up 2 (b); set up 3 (c); set up 4 (d); set up 5 (e).

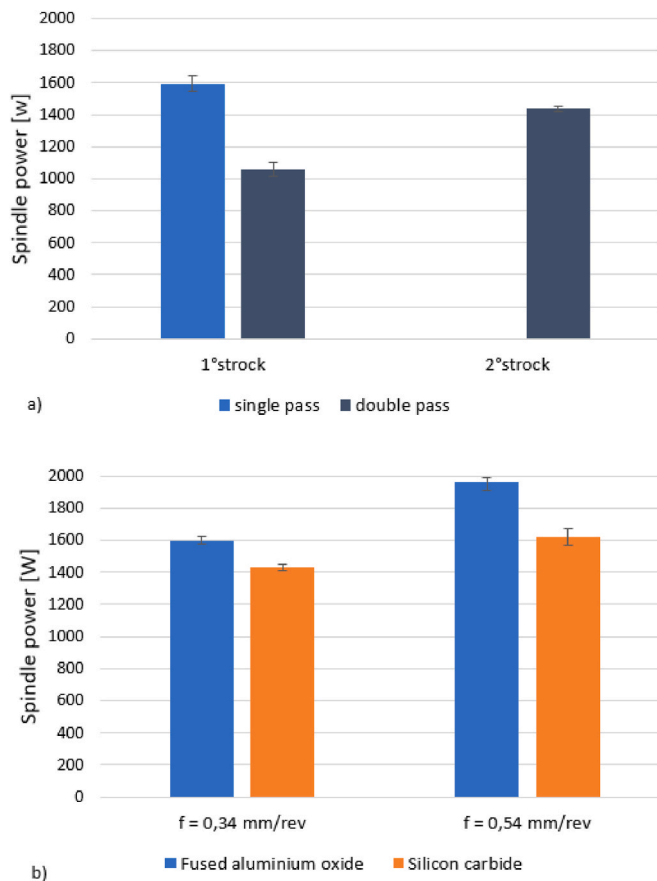


Fig. 10. Spindle power acquisition: comparison between single and double pass (a) and fused aluminium oxide and silicon carbide wheels (b). (For interpretation of the references to colour in this figure legend, the reader is referred to the Web version of this article.)

influenced the thermal effect induced on the gear flank surfaces. Higher the hardness of the binder higher the strength of the wheel to maintain close the worn abrasive grains. The wear of the abrasive grains represents indeed the principal reason of an incorrect grinding operation.

Microstructure analysis by means of scanning electron microscope (SEM) could investigate in detail the different microstructure configuration and agree with the previous microstructural analysis. Fig. 9 a-b-c showed the microstructure resulting from the use of the aluminium oxide wheel, with the lowest and highest feed rate and with the double pass. Martensite microstructure with its typical acicular grains is visible up to the flank surface without defects. Fig. 9 d-e reported the detailed microstructure related to the gears ground with the silicon carbide wheel and it was clear the white layer presence, characterized by a featureless microstructure towards the flank due to the high deformation suffered by the surface (Liao et al., 2021). A marked white layer was shown with highest feed rate value, because the highest feed rate contributes to increase the abrasives wear. Microstructural analysis revealed the different wheels' applicability on the gear dry grinding process. Even though in all the cases good agreement between drawing geometry and the real ground surface dimensional measurements was shown, silicon carbide wheel was not able to reach the microstructural target. Since silicon carbide generally allows better quality process in terms of cutting performance, this result reveals that at equal grain size, the binder grade seems to be more influent than the wheel structure characteristics in dry grinding. Against a substantial increase in porosity volume, that change from 11 with the fused aluminium oxide to 18 with the silicon carbide wheel, a slightly decrease in the binder grade from the designation J of the silicon carbide wheel to H of the fused

aluminium oxide wheel, allows to avoid thermal defects on the gear surfaces within dry grinding process.

Surface integrity results were correlated to on-line spindle power detections. In Fig. 10 a, the spindle power values acquired within fused aluminium oxide wheel application were reported for the single pass and the double pass showing that with the double pass the load could be distributed in two steps reducing the maximum spindle power value. Fig. 10 b reported the spindle power comparison between the wheels in function of the feed rate. The fused aluminium oxide wheel reached the higher values of spindle power for both feed rate, although the microstructural outcomes. Moreover, it was noticed that though the fused aluminium oxide wheel with the lowest feed rate reached the same spindle value of the silicon carbide wheel with the highest feed rate, microstructural results showed very different situations, suggesting that the silicon carbide with high porosity presents a global lower thermal conductivity.

4. Conclusions

Dry grinding process is an innovative technology, recently introduced in the gear production, that could achieve the same quality target compared with the wet grinding process by reducing production costs and environmental pollution. In this paper a surface integrity evaluation within dry grinding process on automotive gears was presented. Grinding tests were performed to analyze the effect of grinding wheel with different specification on different feed rate values and the application of single pass compared to the double pass. Both single and double pass using a fused aluminium oxide wheel could reach a microstructure without thermal defects, but the single pass allows to obtain almost comparable roughness values with a reduction in production time. Considering the effect of the feed rate, an increase of the feed rate increase in the profile and helix error and roughness. Moreover, with the same wheel specification a highest feed rate value could cause thermal defects on the gear flanks surface. Between the fused aluminium oxide and silicon carbide wheels, different feasibility outcomes were revealed. Even though, the silicon carbide wheel was characterized by a higher porosity and was correlated to lower spindle power values, it showed a worst behaviour in terms of grinding burns occurrence. This suggests that in dry grinding the binder assumes a higher influence compare to the structure.

Declaration of competing interest

The author confirm the absence of conflict of interests.

Acknowledgments

Financial support from the European Commission for the European project FATECO (proposal number: 847284 Call: RFCS-2017) is gratefully acknowledged. Moreover, the authors would like to thank EMAG for the technical support that made this study possible.

References

- AGMA 915-1-A02, 2002. *Inspection Practices - Part 1. Cylindrical Gears - Tangential Measurements*, p. 46.
- Chen, X., Opoz, T.T., Oluwajobi, A., 2017. Analysis of grinding surface creation by single-grit approach. *J. Manuf. Sci. Eng. Trans. ASME* 139 (12), 1–10. <https://doi.org/10.1115/1.4037992>.
- Guerrini, Giacomo, Landi, Enrico, Peiffer, Klaus, Fortunato, Alessandro, 2018. Dry grinding of gears for sustainable automotive transmission production. *J. Clean. Prod.* 176, 76–88. <https://doi.org/10.1016/j.jclepro.2017.12.127>.
- Guerrini, Giacomo, Lerra, Flavia, Fortunato, Alessandro, 2019a. The effect of radial infeed on surface integrity in dry generating gear grinding for industrial production of automotive transmission gears. *J. Manuf. Process.* <https://doi.org/10.1016/j.jmapro.2019.07.006>.
- Guerrini, Giacomo, Lutey, Adrian H.A., Melkote, Shreyes N., Ascari, Alessandro, Fortunato, Alessandro, 2019b. Dry generating gear grinding: hierarchical two-step

- finite element model for process optimization. *J. Manuf. Sci. Eng. Trans. ASME* 141 (6), 1–9. <https://doi.org/10.1115/1.4043309>.
- Gupta, Kapil, Laubscher, R.F., Davim, J. Paulo, Jain, N.K., 2016. Recent developments in sustainable manufacturing of gears: a review. *J. Clean. Prod.* 112, 3320–3330. <https://doi.org/10.1016/j.jclepro.2015.09.133>.
- He, Baofeng, Wei, Cui'e, Ding, Siyuan, Shi, Zhaoyao, 2019. A survey of methods for detecting metallic grinding burn. *Measurement: J. Int. Meas. Confed.* 134, 426–439. <https://doi.org/10.1016/j.measurement.2018.10.093>.
- Jermolajev, Stepan, Brinksmeier, Ekkard, Heinzel, Carsten, 2018. Surface layer modification charts for gear grinding. *CIRP Ann.* 67 (1), 333–336. <https://doi.org/10.1016/j.cirp.2018.04.071>.
- Karpuschewski, B., Knoche, H.J., Hipke, M., 2008. Gear finishing by abrasive processes. *CIRP Ann. - Manuf. Technol.* 57 (2), 621–640. <https://doi.org/10.1016/j.cirp.2008.09.002>.
- Kotthoff, Gerd, 2018. NVH Potential of PM Gears for Electrified Drivetrains. *Gear Technology* no. October: 4. https://www.geartechnology.com/articles/0918/NVH_Potential_of_PM_Gears_for_Electrified_Drivetrains/.
- Landi, Enrico, 2016. Changing the game with an innovative machine concept : dry hard-gear finishing. *Gear Sol.* 48–51.
- Liao, Zhirong, la Monaca, Andrea, Murray, James, Alistair Speidel, Ushmaev, Dmitrii, Adam, Clare, Axinte, Dragos, M'Saoubi, Rachid, 2021. Surface integrity in metal machining - Part I: fundamentals of surface characteristics and formation mechanisms. *Int. J. Mach. Tool Manufact.* 162 (December 2020) <https://doi.org/10.1016/j.ijmactools.2020.103687>.
- Liverani, E., Sorgente, D., Ascari, A., Scintilla, L.D., Palumbo, G., Fortunato, A., 2017. Development of a model for the simulation of laser surface heat treatments with use of a physical simulator. *J. Manuf. Process.* 26, 262–268. <https://doi.org/10.1016/j.jmapro.2017.02.023>.
- Mallipeddi, D., Norell, M., Sosa, M., Nyborg, L., 2019. The effect of manufacturing method and running-in load on the surface integrity of efficiency tested ground, honed and superfinished gears. *Tribol. Int.* 131 (November 2018), 277–287. <https://doi.org/10.1016/j.triboint.2018.10.051>.
- Mayer, John E., Angie, H. Price, Purushothaman, Ganesh K., Dhayalan, Arun Kumar, Pepi, Marc S., 2002. Specific grinding energy causing thermal damage in helicopter gear steel. *J. Manuf. Process.* 4 (2), 142–147. [https://doi.org/10.1016/S1526-6125\(02\)70140-0](https://doi.org/10.1016/S1526-6125(02)70140-0).
- Oliveira, J.F.G., Silva, E.J., Guo, C., Hashimoto, F., 2009. Industrial challenges in grinding. *CIRP Ann. - Manuf. Technol.* 58 (2), 663–680. <https://doi.org/10.1016/j.cirp.2009.09.006>.
- Sampaio, Alves, Otávio Barreto De, Luis, De Souza Ruzzi, Rodrigo, Batista Da Silva, Rosemar, Jackson, Mark J., Eduardo Tarrento, Gilson, De Mello, Hamilton José, Roberto De Aguiar, Paulo, Bianchi, Eduardo Carlos, 2017. Performance evaluation of the minimum quantity of lubricant technique with auxiliary cleaning of the grinding wheel in cylindrical grinding of N2711 steel. *J. Manuf. Sci. Eng. Trans. ASME* 139 (12), 1–8. <https://doi.org/10.1115/1.4037041>.
- Zhang, Fang yuan, Duan, Chun zheng, Wang, Min jie, Sun, Wei, 2018. White and dark layer formation mechanism in hard cutting of AISI52100 steel. *J. Manuf. Process.* 32 (December 2017), 878–887. <https://doi.org/10.1016/j.jmapro.2018.04.011>.
- Zhou, Weihua, Tang, Jinyuan, Wen, Shao, 2020. Study on surface generation mechanism and roughness distribution in gear profile grinding. *Int. J. Mech. Sci.* 187 (June), 105921 <https://doi.org/10.1016/j.ijmecsci.2020.105921>.